An Extensive Practical Investigation of FPSO-Based MPPT for Grid Integrated PV System Under Variable Operating Conditions With Anti-Islanding Protection

Priyadarshi, Neeraj; Padmanaban, Sanjeevikumar; Kiran Maroti, Pandav; Sharma, Amarjeet

An Extensive Practical Investigation of FPSO-Based MPPT for Grid Integrated PV System Under Variable Operating Conditions With Anti-Islanding Protection

Neeraj Priyadarshi, Sanjeevikumar Padmanaban ⓘ, *Senior Member, IEEE*, Pandav Kiran Maroti, *Student Member, IEEE*, and Amarjeet Sharma

Abstract—**Maximum power point trackers (MPPT) are required in order to obtain optimal photovoltaic power. To achieve this task, an intelligent fuzzy particle swarm optimization (FPSO) MPPT algorithm has been proposed in this paper. Also an inverter control strategy has been gated with a ripple factor compensation-based modified space vector pulse width modulation (SVPWM) method. The proposed system performance is verified under varying sun irradiance, partial shadow, and loading conditions. For load bus voltage regulation, the buck-boost Zeta converter is selected due to least ripple voltage output. The experimental responses verify the efficiency and improved system performance, which is realized through a MATLAB/Simulink interfaced dSPACE DS1104 real-time board. The proposed MPPT and inverter current controller provides high tracking efficiency and anti-islanding protection with superior dynamic control of the system performance by injecting sinusoidal inverter current to the utility grid. The novelty of this paper is experimental implementation and verification of FPSO-based hybrid MPPT as well as modified SVPWM inverter control has neither been discussed nor implemented before using dSPACE platform by the author's best review.**

Index Terms—**Buck-boost Zeta converter, fuzzy particle swarm optimization (FPSO), maximum power point (MPP), photovoltaic (PV) system, space vector pulse width modulation (SVPWM).**

I. INTRODUCTION

BECAUSE of the exhaustion of fossil fuel and the demand for a clean environment, use of nonconventional sources of energy such as PV, wind, geothermal, tidal, fuel cell, biomass, etc. is required. Renewable energies are playing an important role to supply world's power demand. As solar energy is enormous and free, hence photovoltaic (PV) renewable technology is the most acceptable among all renewable power generation processes [1]–[3]. The existing solar system has deficient conversion efficiency to get electricity generation. Hence, the extraction of maximum power from solar panel can be done by operating the controller under maximum power point trackers (MPPT) mode. Using MPPT algorithms, the tracking efficiency of solar panel is increased and optimum power is obtained from solar panel [4], [5].

Many MPPT techniques along with their detailed implementation and working principles have been reported in the literature. Among them, the hill climbing (HC), incremental conductance (INC) technique, and perturb and observe (P&O) are the most popular and commercially used techniques [6], [7]. However, the major drawbacks of HC/P&O are occasional deviations from the maximum power point (MPP) during variable atmospheric states and calculation of correct perturbation size for the satisfaction of rapid output fulfillment. INC technique is as accomplished as HC/P&O with better out-turn under varying weather situations, but it suffers from perturbation size problems with complex and costly control circuits. Variable perturbation step size is used with adaptive techniques to overcome this drawback. Researchers have considered fuzzy logic controller (FLC) as an effective tool which depends on expertise and it provides solutions to uncertainties and nonlinearity problems [8]. However, due to the existence of multiple maxima on a *P–V* curve, the FLC MPPT controller is unable to track MPP under transient weather conditions. Alternatively, the evolutionary algorithms are the best solution to find an optimal result in the nonlinear problems. The stochastic genetic algorithm based MPPT provides no guarantee to obtain global MPP and has design complexity to find fitness rate under abrupt and partial weather conditions [9]. Moreover, the population-based optimized firefly algorithm has more computational complexity for each iteration which depends on movement of lighting firefly [10]. The artificial bee colony is another optimizing MPPT algorithm discussed in the literature [11]. This bioinspired MPPT method has disadvantages such as fall on local maxima, high cost, difficult design methodology, and limited control variables. The major drawback of conventional particle swarm optimization (PSO) algorithm is adjustment of extra parameters which makes the computational convergence speed slow. Because of randomness presence in acceleration factor, the PSO technique has more MPP tracked period for substantial search areas [12], [13].

With respect to conventional dc–dc converter, Zeta buck-boost converter is selected for this work to give a low voltage ripple [14]. The two-stage PV grid system presented here provides active/reactive power compensation as well as low total

harmonic distortion (THD) in inverter current. Hence, the proposed controller is efficient to control power factor (PF) and current injected to the utility grid. By varying the PF under precise range, the injected reactive power can be dynamically changed and controlled.

Several control methods has been exploited for gating pulse generation of inverter control such as predictive current controller [15], the Hysteresis current controller (HCC) [16], sine pulsewidth modulation (SPWM) [17], etc. Predictive controller method determines the inverter voltages required to force the measured currents which follow the current reference with a fixed switching frequency. Moreover, the system response is affected by the load which makes this current control strategy complex with slow dynamic behavior. With the hysteresis method of current control, the error is compared with the hysteresis band boundaries for generation of switching pulses for inverter. The main advantage of this method is fast and robust dynamic response. The main disadvantage of conventional HCC is variable switching frequency because it has fixed hysteresis band. In the SVPWM method, a simple mapping strategy has been used for generation of switching signal to the inverter to control three-phase inverter voltages [18]–[21]. The major advantage of this method is fixed switching patterns, large linear modulation range, low switching losses, and lesser harmonic distortion compared to other methods of inverter current control. Generated PV power is fed to the utility grid through inverter at the point of common coupling. Based on the load requirement, the power has been balanced between inverter and electric grid. Meanwhile, during transfer of power from PV to a utility grid, protection is required to prevent inverter and load under abnormal operating conditions. During grid failure/fault situations, an anti-islanding method should be employed. Under these situations, the electric grid is cutoff from the inverter and delivers power to local load which prevents unwanted destruction. Compared to passive methods, the active methods will provide complete reliability from islanding protection [22], [23]. In this work, frequency shifting protection scheme for anti-islanding has been employed, which satisfy IEEE, IEC grid codes.

Saufi *et al.* [24] have discussed MATLAB-based analysis of fuzzy PSO (FPSO) for maximum tracking of PV power for a standalone system. In this work, we have not interpreted the experimental PV system performance investigation during variable operating conditions. Lal and Singh [25] have tested PSCAD-based PV utility with PSO MPPT. Reactive power control and utilization of dc link have also been discussed in this work. However, practical performance evaluation has not been discussed under abnormal weather and loading conditions. Saedi *et al.* [26] have proposed PSO-based MPPT with phase locked loop (PLL) for power quality improvement. In this work, dynamic behavior of the PV system have been realized with SVPWM linear current control. Nevertheless, steady and dynamic responses have been demonstrated through only simulation environment. Experimental justification of PSO with SVPWM current control is missing in this work.

In conventional SVPWM control, constant dc bus with zero ripples is not assured at PV output. This paper proposes an
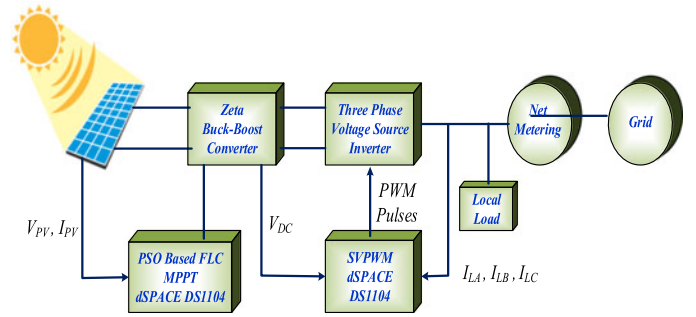

Fig. 1. Complete proposed solar system block diagram.

intelligent FPSO-based MPPT scheme which effectively utilizes modified SVPWM based ripple effect for a two-stage grid integrated PV system responsible for minimization of ripple effect of dc bus voltage. Modified SVPWM control employed for updation and compensation of dc bus voltage generate quality inverter ac output. Therefore, there is no requirement of external ripple compensator filter with bulky size, raised losses, and idle response.

The hybrid FPSO-based MPPT optimizes the input and output membership function by automatic adjustment of fuzzy parameters to generate the optimal duty ratio to power the switch of the dc–dc converter. Unlike conventional control, the proposed strategy is also simple to implement and has reduced switching losses. Using the proposed control strategy, the THD of inverter voltage and current is found better as compared to similar work [27]. This scheme is simple, cheaper with fast tracking speed, and also does not require mathematical model.

The novelty and innovation of this work is that the PV system with a hybrid FPSO MPPT and modified SVPWM based on ripple control has been experimentally studied under anti-islanding protection. The performance of the PV system has been tested under highly fluctuating weather conditions and partial shading conditions as well. This type of PV controller with dSPACE platform has neither been discussed before by our elite assessment.

II. PROPOSED PV SYSTEM DESCRIPTIONS

The complete schematic structure of a PV grid power generation is depicted in Fig. 1, which comprises fuzzy PSO MPPT and modified SVPWM-based inverter controller. The PWM gating signal has been generated for the dc–dc converter to track optimal power from the PV array. The fuzzy PSO MPPT controller has PV voltage and current as input feedback, which produces an optimal duty ratio corresponding to maximum power generation. The zeta converter works as an impedance balancer. The three-phase inverter acts as an interface between the dc link and the utility grid.

A. PV Module Characteristics

PV modules have been constructed using the PV cell modeling comprising the effects of insolation and ambient temperature as shown in Fig. 2. Figs. 3 and 4 show the *I–V* and *P–V* characteristics of the PV panel during different irradiance levels

This article has been accepted for inclusion in a future issue of this journal. Content is final as presented, with the exception of pagination.

PRIYADARSHI *et al.*: EXTENSIVE PRACTICAL INVESTIGATION OF FPSO-BASED MPPT FOR GRID INTEGRATED PV SYSTEM UNDER 3

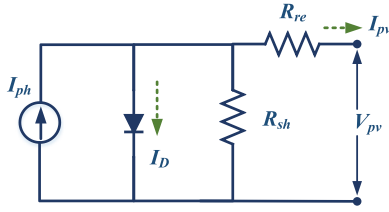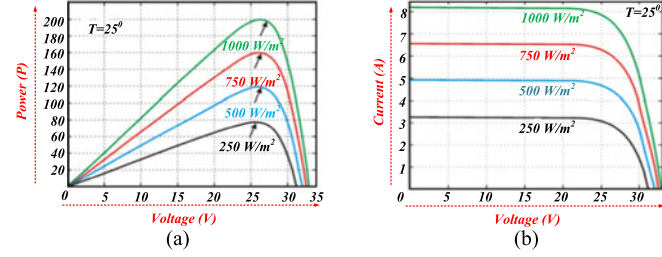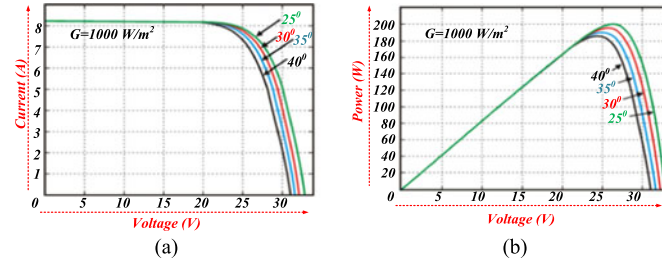
Fig. 2. PV equivalent cell.

Fig. 3. Responses of PV array at varying irradiance and constant ambient temperature. (a) *I–V* Characteristics. (b) *P–V* Characteristics.

Fig. 4. Responses of PV array at constant irradiance and variable ambient temperature. (a) *I–V* Characteristics. (b) *P–V* Characteristics.

TABLE I
PARAMETERS OF 200 W KYOCERA KD200GXLPU PV PANEL

S.N.	Parameter	Value
1	Maximum Power	200 W
2	Max. Voltage	26.6 V
3	Max. current	7.52 A
4	Open circuit voltage	33.2 V
5	Open circuit current	8.36 A

and variable temperatures. The MATLAB/Simulink model is developed based on basic equivalent circuit equations of PV cell, including the variable irradiance and temperature effects.

Table I shows the specifications of PV module used during experimentation.

The PV equivalent cell shown in Fig. 2 is modeled using a current source connected to an anti-parallel diode which is formed by the p-n junction semiconductor that depends on level of irradiance, load current, and ambient temperature. The mathematical equations governing the PV cell V-I characteristics are expressed as follows:

$$I_{\mathrm{ph}} = I_{\mathrm{Diode}} + I_{\mathrm{PV}} + \frac{V_{\mathrm{PV}} + R_S \times I_{\mathrm{PV}}}{R_{\mathrm{SH}}} \tag{1}$$

$$I_{\mathrm{Diode}} = I_{\mathrm{sat}} \left(e^{\frac{V_{\mathrm{Diode}}}{V_{\mathrm{Tem}}}} - 1 \right) \tag{2}$$

$$V_{\mathrm{Diode}} = V_{\mathrm{PV}} + R_S \times I_{\mathrm{PV}} \tag{3}$$

$$V_{\mathrm{Tem}} = \frac{N \times K \times T_m}{Q} \tag{4}$$

where

I_{ph}	Photon current.
I_{Diode}	Diode current.
I_{PV}	Photovoltaic cell current.
V_{PV}	Photovoltaic cell voltage.
R_S	Series resistance.
R_{sh}	Parallel resistance.
I_{Sat}	Saturation current of the diode.
V_{Tem}	Temperature voltage.
V_{Diode}	Voltage across the diode.
N	Quality factor of material at junction.
K	Boltzman constant.
T_m	Measured Temp..
Q	Charge of the electron.

B. PSO Fuzzy Logic Based MPPT Controller

The intelligent MPPT controllers are failing to track peak power when multiple global points exist on a *P–V* curve. For getting an optimal solution to this problem, fuzzy PSO technique is proposed due to adjustment of very less parameters, which makes the optimized membership function with enhanced system performance under variable ambient conditions. In this method, the fuzzy sets are employed to overcome nonlinearity and uncertainty which provide effective control of the plant variables. The hybrid PSO-FLC algorithm optimizes the Mamdani membership functions which adjust the duty ratio of zeta converter automatically under variable weather conditions. The proposed MPPT controller tracks optimal power from the PV module and has zero power oscillation around MPP. Compared to the conventional P&O method of MPPT, FLC-PSO controller output performs under large irradiance fluctuations, convergence of which mainly depends on random velocity factors. The classical HC and P&O MPPT algorithms are based on slope of the *P–V* curve. The power oscillation around MPP has been obtained always with these conventional methods because of reference voltage step variations.

1) Particle Swarm Optimization: The PSO is based on a stochastic evolution theorem which is used to find the simulation of a bird flock's choreography that is able to solve optimization problems. Based on the particle's position and velocity, the fitness function is calculated. It was discovered by Kennedy and Eberhart in 1995. It acts as a global evolutionary optimization process. The method was inspired by the movement of particles in a multidimensional plane called swarm which provides the best optimal solution. The optimal solution can be obtained by employing meta heuristic PSO-based optimized method which works on velocity and position update. Based on previous position best ($P_i(T)$) and global best ($G_i(T)$) parameters, the particle has been accelerated. The new position velocity can be obtained

This article has been accepted for inclusion in a future issue of this journal. Content is final as presented, with the exception of pagination.

4   IEEE SYSTEMS JOURNAL

in all iterations with the help of the previous best. A new iteration can be calculated until the error is minimized and particles can reach at an optimal position. The application of the PSO algorithm was first time realized by a PV MPPT system in 2004. The swarm's particle is associated with two variables as position X(T) and the velocity vector Vi(T) in which Xi1(T), Xi2(T) . . . .Xid(T) are the positions of each particle

where

d   Multidimensional search plane.
i   Each particle index number in swarm.
T   Number of iteration.

The next particle position in a multidimensional search space can be calculated with the help of current position vector Xi(T),velocity vector Vi(T), and best global vector Gi(T) mathematically as follows:

$$V_i(T+1) = \omega(T) \times V(T) + K_1 R_1 \left[P_i(T) - X_i(T)\right]$$
$$+ K_2 R_2 \left[G_i(T) - X_i(T)\right] \quad (5)$$

where

K_1 and K_2 Acceleration constant.
ω(T)   Inertia weight factor.
P_i(T)   Personal best.
G_i(T)   Global best.

The update position vector can be expressed mathematically as follows:

$$X_i(T+1) = X_i(T) + V_i(T+1). \quad (6)$$

The inertia weight is explained as

$$\omega(T) = \frac{\text{Iteration}_{\max} - \text{Iteration}_{\text{current}}}{\text{Iteration}_{\max}} \quad (7)$$

where

Iteration$_{\max}$ Maximum iteration cycle.
Iteration$_{\text{current}}$ Current iteration cycle.

The evaluation function (EF) for individual particle can be calculated mathematically as

$$\text{EF} = \int_0^{T_F} \left[P_{\text{Peak}}(T) - P_{\text{PV}}(T)\right]^2 dT \quad (8)$$

where

P_{Peak} Maximum power, delivering capacity of PV panel under standard test condition.
T_F Total period of simulation.

Acceleration constants (K_1, K_2) perform the particle velocity toward personal and global best locations. A particle with minor acceleration factor has far away movement from target. On the other hand, target movement of a particle takes place with a high acceleration factor. The optimization with high convergence speed is obtained at $K_1 = K_2 = 2$ by heat and trial process. The complete PSO fuzzy process is realized using MATLAB through the flowchart which is presented in Fig. 6. Table II presents the PSO parameters specification used in this work. The considered PV system is denoted by the fitness function. On the other hand, duty cycle and its incremental variations are denoted by particle position and velocity, respectively. The fitness function is used to find the accurate performance of the
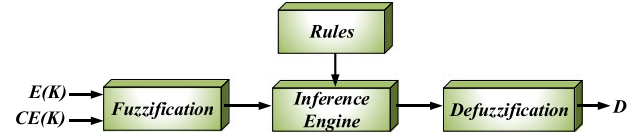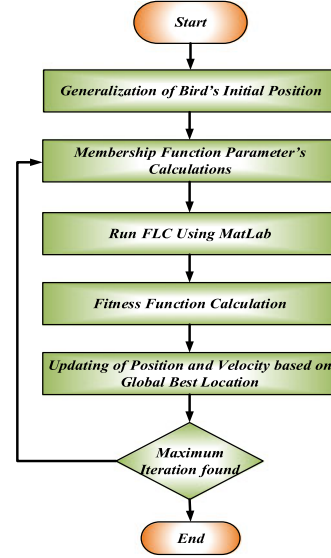

Fig. 5.   Block diagram of a FLC.

Fig. 6.   Flowchart of a PSO-based FLC MPPT algorithm.

TABLE II
PSO SPECIFICATION

S.N.	Parameter	Value
1	Inertia weight factor	0.5
2	Self Confidence inertia weight factor (K_1)	1.5 to 2
3	Swarm confidence (K_2)	2 to 2.5
4	Frequency deviation (df)	0.007
5	Size of population	50

system which is associated with frequency deviation (df). It denotes the power system efficient behavior and can be expressed mathematically as follows:

$$\text{Fitness Function (FF)} = \int |df| \, dT \quad (9)$$

where df = Frequency deviation.

2) Fuzzy Logic Controller: FLC algorithm is employed for tracking maximum power because it gives a better dynamic response, high convergence rate, and it is easy to implement unlike traditional MPPT controllers. The fuzzy MPPT controller extracts utmost power from the PV system at variable irradiance and ambient temperatures. Fig. 5 shows the basic structure of the adopted FLC which comprises fuzzification, inference engine, and defuzzification components.

1) Fuzzification: The two FLC inputs are the errors, i.e., E(q) (input1) and change of error CE(q) (input2), and can be obtained by following relations:
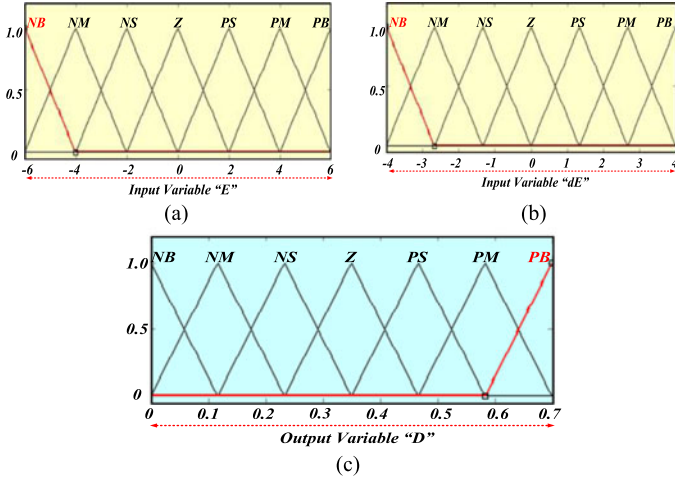
This article has been accepted for inclusion in a future issue of this journal. Content is final as presented, with the exception of pagination.

PRIYADARSHI *et al.*: EXTENSIVE PRACTICAL INVESTIGATION OF FPSO-BASED MPPT FOR GRID INTEGRATED PV SYSTEM UNDER

5

Fig. 7. Membership functions. (a) Input variable (E). (b) Input variable (dE). (c) Output variable (D).

TABLE III
FUZZY RULE BASE

E / dE	NB	NM	NS	Z	PS	PM	PB
NB	Z	Z	Z	PB	PB	PB	PB
NM	Z	Z	Z	Z	Z	Z	Z
NS	Z	Z	Z	PS	PS	PS	PS
Z	PS	PS	Z	Z	Z	Z	NS
PS	NS	NS	NS	NS	Z	Z	Z
PM	NS	NS	Z	Z	NS	NM	NS
PB	NB	NB	NB	NB	Z	NB	Z

$$E(q) = \frac{P_{\mathrm{PV}}(q) - P_{\mathrm{PV}}(q-1)}{V_{\mathrm{PV}}(q) - V_{\mathrm{PV}}(q-1)} \tag{10}$$

$$CE(q) = E(q) - E(q-1) \tag{11}$$

where P_{PV} (q) and V_{PV} (q) are the power and voltage of the PV array, respectively. The differentiation of P(q) with respect to V(q) is obtained by (10) and (11) which act as an input to the FLC. The defuzzification output duty cycle (D) gives trigger pulses to the Zeta converter to operate the PV panel at MPPT. The input and output variables are assigned with seven linguistic variables as shown in Fig. 7. In the current paper, triangular fuzzy rules are adopted compared with trapezoidal, Gaussian, and sigmoid functions because the proposed MATLAB/Simulink model converges easily with simpler arithmetic operation, and require less data for membership function decision. Mamdani's method is used as a fuzzy decision rule base which is based on the max–min composition. The 49 fuzzy rules are constructed as depicted in Table III.

1) *Defuzzification:* For the defuzzification, the centroid method is applied to generate an actual duty cycle to trig-

ger zeta converter. Generated PWM pulses are fed to gate terminal of power switch of zeta converter.

III. MODIFIED SVPWM INVERTER CONTROLLER

In this work, modified SVPWM controller has been employed which minimizes the ripple effect of dc bus voltage. Various inverter states are dependent on ripple factor which is responsible for update and compensation of dc bus voltage and generate quality inverter ac output. Therefore, there is no requirement of external ripple compensator filter with bulky size, raised losses, and idle response. In conventional SVPWM control, constant dc bus with zero ripples is not assured at PV output.

Compared to other PWM methods of generation of switching signal to the power switches of VSI, the SVPWM is the most predominant method due to its less harmonic distortion, fixed switching pattern, small switching losses, fast dynamic, and precise response performance. The three-phase voltage is converted into α–β reference frame as follows:

$$\begin{bmatrix} V_\alpha \\ V_\beta \end{bmatrix} = \begin{bmatrix} 1 & \frac{1}{2} & -\frac{1}{2} \\ 0 & \frac{\sqrt{3}}{2} & -\frac{\sqrt{3}}{2} \end{bmatrix} \begin{bmatrix} V_A \\ V_B \\ V_C \end{bmatrix}. \tag{12}$$

The d–q frame grid voltage is expressed as

$$\begin{bmatrix} V_d \\ V_q \end{bmatrix} = \begin{bmatrix} \cos(\theta) & \sin(\theta) \\ -\sin(\theta) & -\cos(\theta) \end{bmatrix} \begin{bmatrix} V_\alpha \\ V_\beta \end{bmatrix}. \tag{13}$$

The three-phase output is obtained after rotation of reference vector (V_{REF}) at angular frequency ω which provides switching between six active and two zero vectors. The reference voltage sector is evaluated mathematically as follows:

$$V^*_{\mathrm{REF}_1} = V_\beta \tag{14}$$

$$V^*_{\mathrm{REF}_2} = \frac{\sqrt{3}}{2}V_\alpha - \frac{1}{2}V_\beta \tag{15}$$

$$V^*_{\mathrm{REF}_3} = -\frac{\sqrt{3}}{2}V_\alpha - \frac{1}{2}V_\beta. \tag{16}$$

Also

$$\text{If } V^*_{\mathrm{REF}_1} > 0 \Rightarrow A = 1 \text{ or } A = 0 \tag{17}$$

$$\text{If } V^*_{\mathrm{REF}_2} > 0 \Rightarrow B = 1 \text{ or } B = 0 \tag{18}$$

$$\text{If } V^*_{\mathrm{REF}_3} > 0 \Rightarrow C = 1, \text{ or } C = 0. \tag{19}$$

The sector mapping (S_{mapping}) has six integral values from 1 to 6 and expressed mathematically as

$$S_{\mathrm{mapping}} = A + 2B + 4C. \tag{20}$$

The six active and two zero vectors are named as $(V_1$ to $V_6)$ and $(V_0$ and $V_7)$, respectively, and angle between two active vectors is found to be 60°, which is responsible to provide electrical power to the load. Moreover, the two zero vectors fed zero power to the load because these vectors are situated at the origin. The SVPWM has total eight switching patterns which are used to find voltage space vector. It consists of six active space vector with 2/3 V_{DC} amplitude and two zero vectors. To reduce the switching period and current harmonic content, the reference voltage has been calculated with the help of adjacent
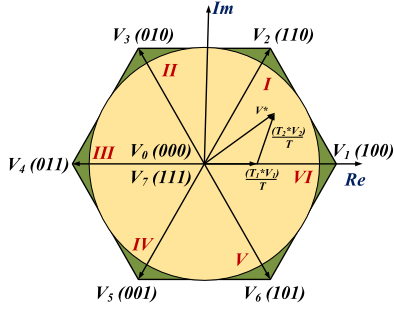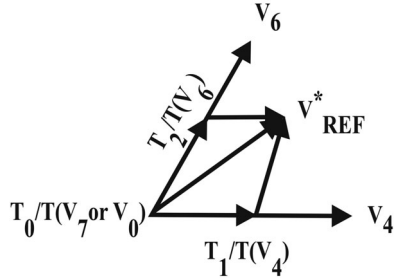
Fig. 8.   SVPWM sectors.

Fig. 9.   Resultant voltage vector.

vector. Figs. 8 and 9 depict SVPWM sector and resultant voltage vector using adjacent vector, respectively

$$V_{\mathrm{REF}}^{*} = \frac{T_1}{T} \times V_{\mathrm{DC}} + \frac{T_2}{T} \times V_{\mathrm{DC}} \times e^{\frac{j\pi}{3}}. \quad (21)$$

And

$$T_1 = \frac{V_{\mathrm{REF}}^{*}}{V_{\mathrm{DC}}} \times T \left[\mathrm{Cos}(\theta) - \frac{1}{\sqrt{3}} \mathrm{Sin}(\theta) \right]$$

$$= \frac{2 V_{\mathrm{REF}}^{*}}{\sqrt{3} \times V_{\mathrm{DC}}} \times T \times \mathrm{Sin}\left(\frac{\pi}{3} - \theta \right) \quad (22)$$

$$T_2 = 2 \times \frac{V_{\mathrm{REF}}^{*}}{\sqrt{3} \times V_{\mathrm{DC}}} \times T \times \mathrm{Sin}(\theta) \quad (23)$$

$$V_{\mathrm{DC}} = R_{\mathrm{ripple}} V_{\mathrm{DC_{actual}}} \quad (24)$$

where
V_{DC} Desired dc bus voltage.
R_{ripple} Ripple Factor.
V_{DCactual} Measured dc bus voltage.

$$T_0 = T - (T_1 + T_2) \quad (25)$$

$$T_0 = T \left[1 - \frac{2 V_{\mathrm{REF}}^{*}}{\sqrt{3} \times V_{\mathrm{DC}}} \times T \times \mathrm{Cos}\left(\frac{\pi}{6} - \theta \right) \right]. \quad (26)$$

The asymmetrical switching period (T_{S1}, T_{S2}, and T_{S3}) of six switches of a three-phase SVPWM based inverter can be calculated as

$$T_A = \frac{1}{2}(T_0 - T_1 - T_2) \quad (27)$$

$$T_B = T_A - T_1 \quad (28)$$

$$T_C = T_B + T_2. \quad (29)$$

TABLE IV
SWITCHING PERIOD OF A THREE-PHASE SVPWM

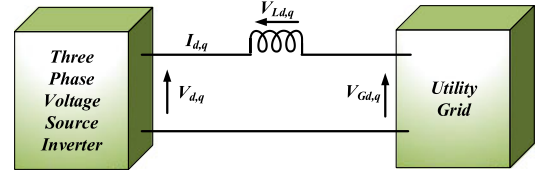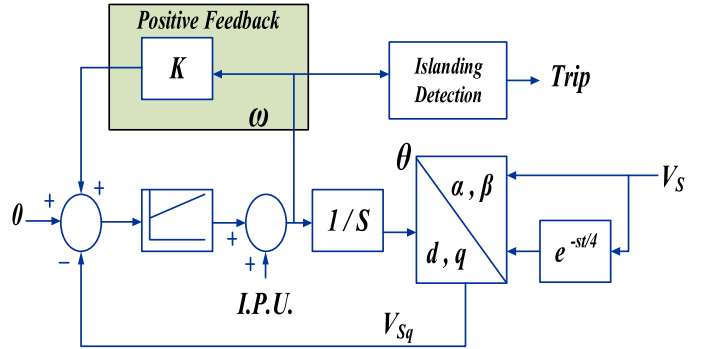| Time	Sector					
	1	2	3	4	5	6
T_{S1}	T_A	T_B	T_C	T_C	T_B	T_A
T_{S2}	T_B	T_A	T_A	T_B	T_C	T_C
T_{S3}	T_C	T_C	T_B	T_A	T_A	T_B

Fig. 10.   VSI and grid connection in d–q reference frame.

Fig. 11.   Control strategy of PLL-based anti-islanding.

Table IV shows the switching period of three-phase SVPWM denoted by T_{S1}, T_{S2}, and T_{S3}, respectively, which represents the switching pattern of each sector. Voltage and current in the d–q frame is written with the reference to Fig. 10 as

$$V_d = V_{Ld} + V_{Gd} \quad (30)$$

$$V_q = V_{Lq} + V_{Gq} \quad (31)$$

where V_{Gd} and V_{Gq} are grid voltage in the d–q stationary frame and ωf is an angular frequency of grid.

A. Islanding Detection

The control strategy of PLL-based anti-islanding is depicted by Fig. 11. The PLL detects the grid voltage phase and frequency and feedback to the grid controller, which provides grid protection and connection. The positive frequency feedback is used to get islanding detection which provides perturbation in phase in case of grid failure. As a result of this, the system is turned automatically OFF and converter frequency varies around 2%, which is known as anti-islanding protection. In the grid connected mode of operation, the converter frequency becomes equal to grid frequency because of small perturbation in converter phase angle.
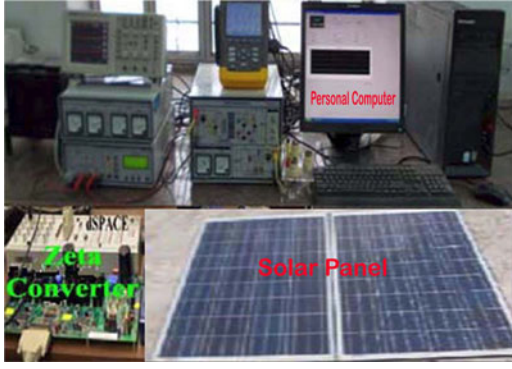
This article has been accepted for inclusion in a future issue of this journal. Content is final as presented, with the exception of pagination.

PRIYADARSHI *et al.*: EXTENSIVE PRACTICAL INVESTIGATION OF FPSO-BASED MPPT FOR GRID INTEGRATED PV SYSTEM UNDER 7

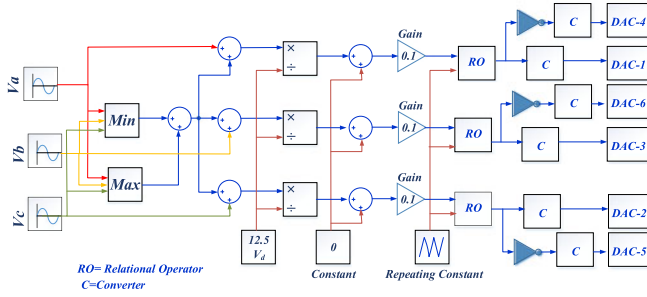Fig. 12. Experimental developed setup of the proposed PV system.

Fig. 13. dSPACE interfaced SVPWM Simulink model.

IV. EXPERIMENTAL RESULTS AND DISCUSSION

A practical setup has been developed to verify the effectiveness of the proposed MPPT and inverter current controller which is depicted in Fig. 12. It comprises PV simulator, zeta converter, dSPACE kit, oscilloscope, and Fluke 43 B power quality analyzer as main components. An ATE-62050H-600S PV emulator with dc programed is employed to find the panel characteristics. A real-time dSPACE DS1104 controller interface is used to perform the system control by conditioning all the field signals. The Simulink model is interfaced with external hardware using a dSPACE platform which is described in Fig. 13. The sine wave output obtained from the control desk is compared with a triangular signal with 10-kHz switching frequency. The inverter gating signals are interfaced with dSPACE through a D/A converter. The simulated design modeling has been implemented in Simulink which is run using a dSPACE DS1104 board. The major elements of the prototype are IGBT, circuit drive, input dc source, three-phase inverter, and a personal computer with dSPACE DS1104. The major advantage of this proposed control is to control the THD, PF, active, and reactive power instantaneously with a high accuracy.

In order to realize the effective performance of a modified SVPWM current controller based grid connected PV system, the experimentation is performed using the MATLAB/Simulink interfaced dSPACE platform. For this purpose, the grid phase voltage is assumed as 230 V with 50-Hz frequency and 420-V dc-link voltages. Fig. 14 shows the practical response of a dc-link voltage. From experimental results, it is clear that the proposed modified SVPWM-based current controller makes better utilization of dc-link voltage. The line and phase voltage
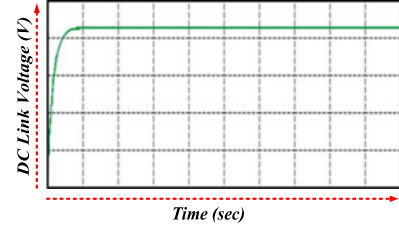

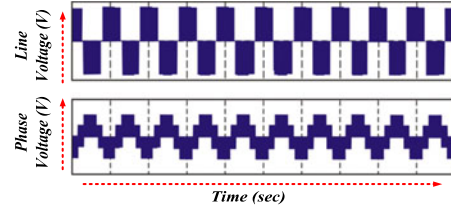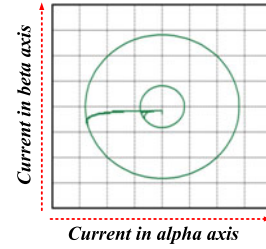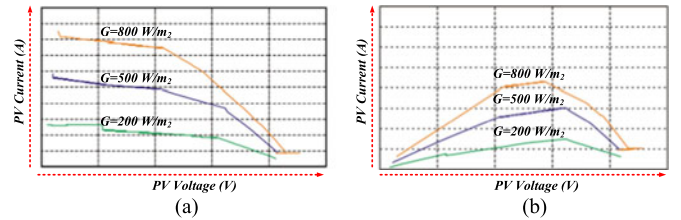Fig. 14. Practical response of dc-link voltage.

Fig. 15. Practical responses of line and phase voltage of a three-phase voltage source inverter.

Fig. 16. Experimental locus of the proposed controller during step load change in α–β stationary reference.

Fig. 17. Characteristics at different irradiance. (a) *I–V.* (b) *P–V.*

of a three-phase voltage source inverter is depicted by Fig. 15 which justifies the effectiveness of the proposed controller. The locus of the proposed controller during step load change in α–β stationary reference frame is depicted in Fig. 16. Practically obtained *I–V* and *P–V* characteristics are depicted in Fig. 17(a) and (b), respectively, under a varying irradiance level.

The comparative practical results depicted in Fig. 18 demonstrate the steady-state performance under utmost power extraction at MPP. The proposed FPSO controller has provided high tracked PV output with zero oscillation with MPP compared to conventional P&O control. The experimentally obtained $V_{\rm PV}$ and $I_{\rm PV}$ resemble the desired values [6], [9].

Fig. 19 demonstrates the experimental responses of the proposed FPSO versus conventional P&O control of PV system under varying loading conditions. These responses illustrate the effective dynamic behavior of the proposed PV MPPT
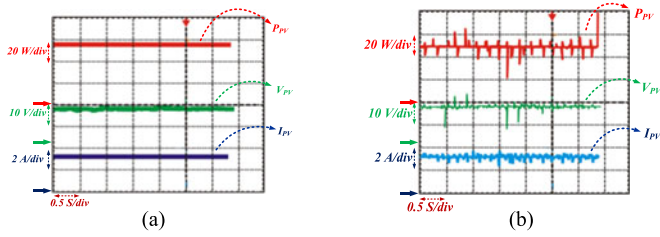
This article has been accepted for inclusion in a future issue of this journal. Content is final as presented, with the exception of pagination.

8   IEEE SYSTEMS JOURNAL

Fig. 18.   Steady-state performance under utmost power extraction at MPP. (a) Proposed FPSO control. (b) Conventional P&O.
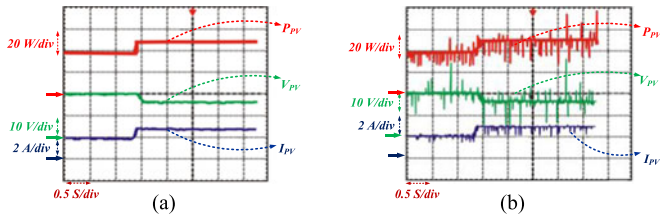

Fig. 19.   Experimental responses of the proposed FPSO versus conventional P&O control of PV system under varying loading conditions.
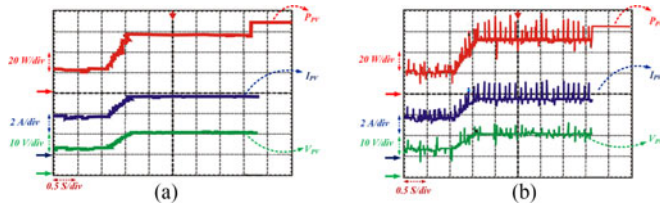

Fig. 20.   Practical PV system behavior under changing sun insolation with fixed loading condition for proposed FPSO versus conventional P&O control.
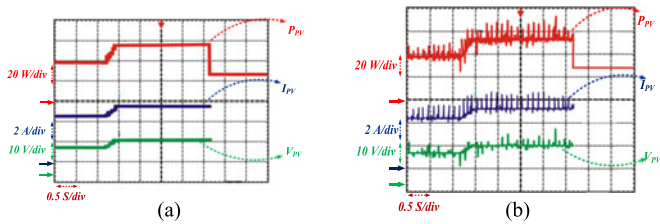

Fig. 21.   PV system behavior with changing surroundings temperature. (a) Proposed FPSO. (b) Conventional P&O control.
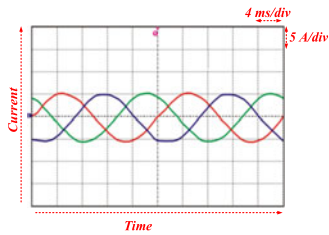

Fig. 22.   Experimental three-phase grid current.

controller. Fig. 20 interprets the practical PV system behavior under changing sun insolation with the fixed loading condition for proposed FPSO versus conventional P&O control of MPPT. With respect to existing MPPT control, FPSO-based MPPT has provided a smooth dynamic response of a PV power system.

The obtained experimental results demonstrate that the MPP is achieved with negligible ripple and has fast and precise
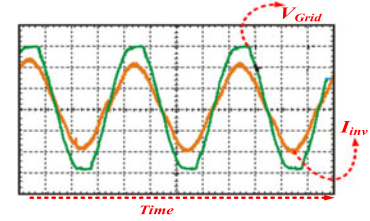

Fig. 23.   Experimental grid voltage and inverter current during steady-state condition.
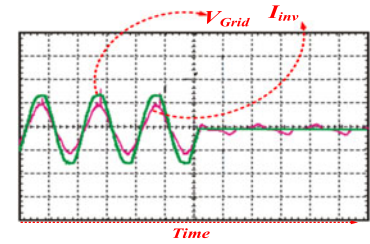

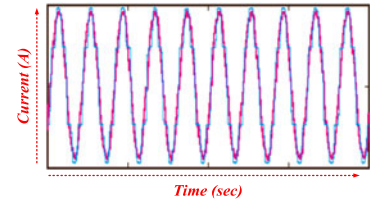Fig. 24.   Islanding condition grid voltage and inverter current.

Fig. 25.   Experimental grid current injected to the utility grid at unity PF operation with proposed (red line) and conventional controllers (blue line).
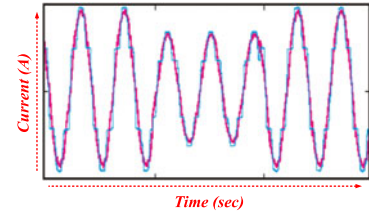

Fig. 26.   Experimental grid current injected to the utility grid at unity PF operation with proposed (red line) and conventional controllers (blue line).
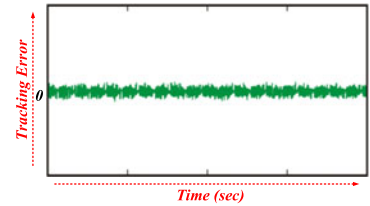

Fig. 27.   Experimental is tracking behavior of the proposed controller.
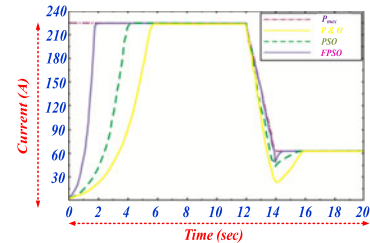

Fig. 28.   Practical tracking efficiency curve of proposed versus conventional control.

This article has been accepted for inclusion in a future issue of this journal. Content is final as presented, with the exception of pagination.

PRIYADARSHI *et al.*: EXTENSIVE PRACTICAL INVESTIGATION OF FPSO-BASED MPPT FOR GRID INTEGRATED PV SYSTEM UNDER
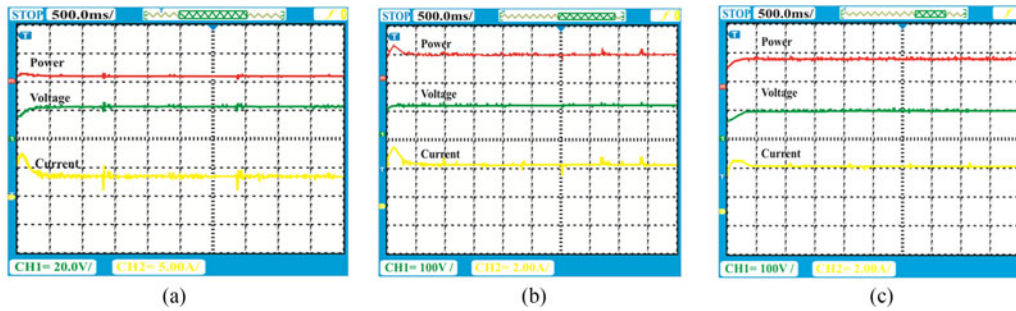9

Fig. 29.   Practical PV system performance under partial shading condition. (a) P&O. (b) PSO. (c) FPSO.
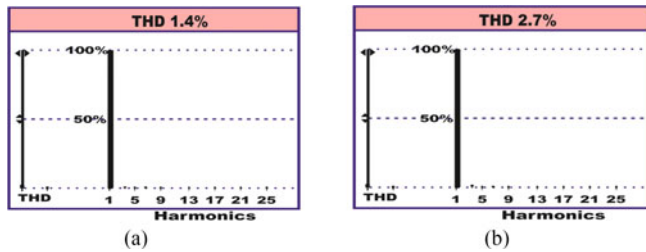
Fig. 30.   THD spectrum of Grid current under (a) steady state and (b) dynamic state.

Fig. 31.   Unity PF operation.

dynamic response with small convergence computational time. The performance of a PV system behavior has been also verified under changing surrounding temperature, which is indicated by Fig. 21 with proposed FPSO versus conventional P&O control. These experimental responses satisfactorily justified the robust dynamic state of the PV system.

The three-phase practical sinusoidal grid current is shown in Fig. 22. Fig. 23 depicts the practically found grid voltage and inverter current which validates the effectiveness of the inverter performance. During islanding condition, i.e., when grid is turned OFF, the experimental response of the grid voltage and inverter current is presented in Fig. 24. When grid voltage reaches a zero crossing position, the power loss is judged by the inverter at time "t." The effectiveness of the proposed controllers has been tested with steady as well as dynamic operating states. Fig. 25 depicts the compared experimental grid current injected into the utility grid at unity PF operation with proposed and conventional controllers. The practical results reveal that the proposed controller makes pure sinusoidal grid current. Also, the operation of proposed controller has been evaluated under variable environmental condition.

Due to change of irradiance level on PV modules, the grid current varies and attains steady-state operation which verifies that the effective system behavior is clearly explained using Fig. 26. The practically found tracking error is depicted in Fig. 27 which interprets the excellent tracked behavior of the propound controller as it approaches zero. The practical tracking efficiency curve of the proposed PSO-FLC versus PSO and P&O MPPT algorithms have been depicted in Fig. 28 which completely validates the accuracy, efficiency, and effectiveness of the proposed controller design. Performance comparison with conventional P&O, PSO, and FPSO MPPT has been discussed and demonstrated on a single graph presented in Fig. 28. The FPSO MPPT method provides high tracking performance compared to PSO
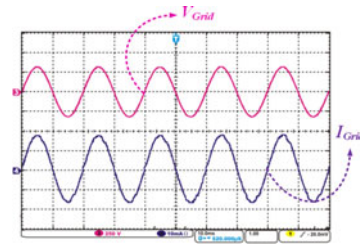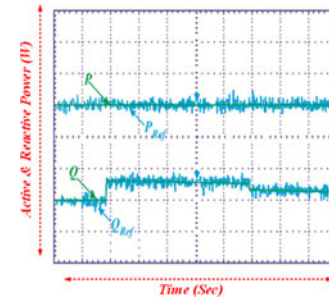

Fig. 32.   Power capability of proposed control system.

and P&O method. The performance of the proposed PV system has been tested under partial shading conditions. Experimental responses depicted in Fig. 29(a), (b), and (c) interpret that FPSO algorithm reaches MPP with zero oscillation and has high tracked efficiency compared to PSO and P&O methods under partial shading conditions.

A modified SVPWM based on ripple control has been employed which provides low THD and is explained with FFT spectrum of grid current under steady-state and dynamic operating conditions which follows the IEEE 519 standard as illustrated in Fig. 30. Unity PF operation with grid voltage and grid current in phase has been depicted and verified using practical results shown in Fig. 31 under a steady-state condition. The injecting power capability of the hybrid FPSO and modified SVPWM inverter control has been explained with obtained practical results shown in Fig. 32 which reveals that active power is maintained constant throughout with controlled reactive power.

V.   CONCLUSION

In this paper, an intelligent PSO FLC based MPPT scheme and modified SVPWM based ripple compensator controller have been developed and tested in a grid-integrated PV system to en-

hance dynamic and steady-state performance with optimized output power. Zeta converter employed effective load voltage regulation with low ripple in the output. The intelligent PSO fuzzy MPPT gives better tracking efficiency under changing environmental conditions. The simulated and practical responses clearly interpret the effectiveness of the propound controller design. The proposed system works without a steady-state error and gives fast and precise tracking ability for varying irradiance level with eliminated oscillations around the MPP compared to conventional controller. The effectiveness of PV system has significantly examined during islanding situations which prevents inverter from abnormal effects and faults. The complete behavior of the proposed controllers is tested and validated through real-time dSPACE DS1104 controller interface under islanding operating conditions.

REFERENCES

[1] J. R. R. Zientarski, M. L. S. Martins, J. R. Pinheiro, and H. L. Hey, "Series-connected partial-power converters applied to PV systems: A design approach based on step-up/down voltage regulation range," *IEEE Trans. Power Electron.*, to be published, doi: 10.1109/TPEL.2017.2765928.

[2] B. Singh, C. Jain, and A. Bansal, "An improved adjustable step adaptive neuron based control approach for grid supportive SPV system," *IEEE Trans. Ind. Appl.*, vol. 54, no. 1, pp. 563–570, Jan./Feb. 2017.

[3] A. Sangwongwanich, Y. Yang, F. Blaabjerg, and D. Sera, "Delta power control strategy for multi-string grid-connected PV inverters," *IEEE Trans. Ind. Appl.*, vol. 53, no. 4, pp. 3862–3870, Jul./Aug. 2016.

[4] P. Sanjeevikumar, G. Grandi, P. W. Wheeler, F. Blaabjerg, and J. Loncarski, "A simple MPPT algorithm for novel PV power generation system by high output voltage DC-DC boost converter," in *Proc. IEEE 24th Int. Symp. Ind. Electron.*, 2015, pp. 214–220, DOI: 10.1109/ISIE.2015.7281471

[5] S. Jain, C. Ramulu, P. Sanjeevikumar, O. Ojo, and A. H. Ertas, "Dual MPPT algorithm for dual PV source fed open-end winding induction motor drive for pumping application," *Eng. Sci. Technol.: Int. J.*, vol. 19, no. 4, pp. 1771–1780, Dec. 2016.

[6] A. M. Noman, K. E. Addoweesh, and H. M. Mashaly, "Simulation and dspace hardware implementation of the MPPT techniques using buck boost converter," in *Proc. IEEE 27th Can. Conf. Electr. Comput. Eng.*, 2014, pp. 1–8.

[7] Z. A. Ghani, A. Mohamed, and M. A. Hannan, "Prototype development of an intelligent power conditioning unit For PV generation system," in *Proc. IEEE Int. Conf. Ind. Technol.*, 2013, pp. 758–763.

[8] A. E. Khateb, N. A. Rahim, J. Selvaraj, and M. N. Uddin, "Fuzzy logic controller based SEPIC converter for maximum power point tracking," *IEEE Trans. Ind. Appl.*, vol. 50, no. 4. pp. 2349–2358, Jul./Aug. 2014. [Online]. Available: http://ieeexplore.ieee.org/stamp/stamp.jsp?tp = &arnumber = 6704722&isnumber = 6855381.

[9] N. Priyadarshi, A. Anand, A. K. Sharma, F. Azam, V. K. Singh, and R. K. Sinha, "An experimental implementation and testing of GA based maximum power point tracking for PV system under varying ambient conditions using dSPACE DS 1104 controller," *Int. J. Renew. Energy Res.*, vol. 7, no. 1, pp. 255–265, 2017.

[10] N. A. Windarko, A. Tjahjono, D. O. Anggriawan, and M. H. Purnomo, "Maximum power point tracking of photovoltaic system using adaptive modified firefly algorithm," in *Proc. Int. Electron. Symp.*, 2015, pp. 31–35.

[11] K. Sundareswaran, P. Sankar, P. S. R. Nayak, S. P. Simon, and S. Palani, "Enhanced energy output from a PV system under partial shaded conditions through artificial Bee colony," *IEEE Trans. Sustain. Energy*, vol. 6, no. 1, pp. 198–209, Jan. 2015. [Online]. Available: http://ieeexplore.ieee.org/stamp/stamp.jsp?tp = &arnumber = 6955814&isnumber = 6983670.

[12] R. B. A. Koad, A. F. Zobaa, and A. El-Shahat, "A novel MPPT algorithm based on particle swarm optimization for photovoltaic systems," *IEEE Trans. Sustain. Energy*, vol. 8, no. 4, pp. 468–476, Apr. 2017.

[13] C. Manickam, G. R. Raman, and G. P. Raman, "A hybrid algorithm for tracking of GMPP based on P&O and PSO with reduced power oscillation in string inverters," *IEEE Trans. Ind. Electron.*, vol. 63, no. 10, pp. 6097–6106, Oct. 2016.

[14] R. Kumar and B. Singh, "BLDC motor driven solar PV array fed water pumping system employing zeta converter," *IEEE Trans. Ind.*

[15] R. Errouissi, A. Al-Durra, and S. M. Muyeen, "Design and implementation of a nonlinear PI predictive controller for a grid-tied photovoltaic inverter," *IEEE Trans. Ind. Electron.*, vol. 64, no. 2, pp. 1241–1250, Feb. 2017. [Online]. Available: http://ieeexplore.ieee.org/stamp/stamp.jsp?tp = &arnumber = 7592909&isnumber = 7812803.

[16] P. K. H. Dost and C. Sourkounis, "Flexible dimensioning opportunities of a (virtual) flux based hysteresis controller for a reduced switching frequency," *IEEE Trans. Ind. Appl.*, vol. 52, no. 4, pp. 3451–3460, Jul./Aug. 2016. [Online]. Available: http://ieeexplore.ieee.org/stamp/stamp.jsp?tp = &arnumber = 7445180&isnumber = 7514285.

[17] Q. Zeng and L. Chang, "An advanced SVPWM-Based predictive current controller for three-phase inverters in distributed generation systems," *IEEE Trans. Ind. Electron.*, vol. 55, no. 3, pp. 1235–1246, Mar. 2008. [Online]. Available: http://ieeexplore.ieee.org/stamp/stamp.jsp?tp = &arnumber = 4391046&isnumber = 4459824.

[18] C. Bharatiraja, S. Babu, V. Krishnakumar, J. L. Munda, and P. Sanjeevikumar, "Investigation of slim type BLDC motor drive with torque ripple minimization using abridged space-vector PWM control method," *Int. J. Power Electron. Drive Syst.*, vol. 8, no. 2, pp. 593–600, Jun. 2017. [Online]. Available: http://www.iaesjournal.com/online/index.php/IJPEDS/article/view/12211/0.

[19] R. Gunabalan, V. Subbiah, and P. Sanjeevikumar, "Vector Control of three-phase parallel connected two motor single inverter speed sensor-less drive," *Turkish J. Elect. Eng. Comput. Sci.*, vol. 24, no. 5, pp. 4027–4041, Jun. 2016. [Online]. Available: journals.tubitak.gov.tr/elektrik/issues/elk-16-24-5/elk-24-5-53-1410-48.pdf.

[20] P. Sanjeevikumar, G. Grandi, O. Ojo, and F. Blaabjerg, "Direct vector controlled six-phase asymmetrical induction motor with power balanced space vector PWM multilevel operation," *Int. J. Power Energy Convers.*, vol. 7, no. 1, pp. 57–83, Feb. 2016. [Online]. Available: http://www.inderscienceonline.com/doi/abs/10.1504/IJPEC.2016.075068.

[21] P. Sanjeevikumar, G. Grandi, F. Blaabjerg, O. Ojo, and P. Wheeler, "Power sharing algorithm for vector controlled six-phase AC motor with four customary three-phase voltage source inverter drive," *Eng. Sci. Technol.: Int. J.*, vol. 18, no. 3, pp. 408–415, Sep. 2015. [Online]. Available: http://www.sciencedirect.com/science/article/pii/S2215098615000324.

[22] A. Ahmad and L. Rajaji, "Anti islanding technique for grid connected residential solar inverter system," in *Proc. Chennai 4th Int. Conf. Sustain. Energy Intell. Syst.*, 2013, pp. 114–118.

[23] I. Mazhari, H. Jafarian, B. Parkhideh, S. Trivedi, and S. Bhowmik, "Locking frequency band detection method for grid-tied PV inverter islanding protection," in *Proc. IEEE Energy Convers. Congr. Expo.*, Montreal, QC, Canada, 2015, pp. 1976–1981.

[24] Y. Soufi, M. Bechouat, and S. Kahla, "Fuzzy controller design using particle swarm optimization for photovoltaic maximum power point tracking," in *Proc. Int. Smart Grid Workshop Certificate Program*, Istanbul, Turkey, 2016, pp. 1–6.

[25] V. N. Lal and S. N. Singh, "Single-stage utility-scale PV system with PSO based MPPT controller," in *Proc. 18th Nat. Power Syst. Conf.*, Guwahati, India, 2014, pp. 1–6.

[26] W. Al-Saedi, S. W. Lachowicz, and D. Habibi, "An optimal current control strategy for a three-phase grid-connected photovoltaic system using Particle Swarm Optimization," in *Proc. IEEE Power Eng. Autom. Conf.*, Wuhan, China, 2011, pp. 286–290.

[27] A. R. Mohanty and A. K. Kapoor, "Performance evaluation of HCC & SVPWM current controllers for shunt APF under fault conditions," in *Proc. India Int. Conf. Power Electron.*, 2011, pp. 1–8.

Neeraj Priyadarshi received the M.Tech. degree in power electronics and drives in 2010 from the Vellore Institute of Technology, Vellore, India, and the Doctorate degree from the Government College of Technology and Engineering, Udaipur, India.

He is currently associated with Millia Institute of Technology, Purnea, India. In previous postings, he was with the JK University, Geetanjali Institute, Global Institute and SS Group, Rajasthan, India. He has published more than 40 papers in journals and conferences. His current research interests include power electronics, control system, power quality, and solar power generation.

Dr. Priyadarshi is a Reviewer of *International Journal of Renewable Energy Research*.

Sanjeevikumar Padmanaban (M'12–SM'15) received the Bachelor's degree in electrical engineering from the University of Madras, Chennai, India, in 2002, the Master's degree (Hons.) in electrical engineering from Pondicherry University, Pondicherry, India, in 2006, and the Ph.D. degree in electrical engineering from the University of Bologna, Bologna, Italy, in 2012.

He was an Associate Professor with Vellore Institute of Technology from 2012 to 2013. In 2013, he was with the Faculty of the National Institute of Technology, Pondicherry, India. In 2014, he was invited as a Visiting Researcher in the Department of Electrical Engineering, Qatar University, Doha, Qatar, funded by the Qatar National Research Foundation (Government of Qatar). He continued his research activities with Dublin Institute of Technology, Dublin, Ireland, in 2014. He was an Associate Professor with the Department of Electrical and Electronics Engineering, University of Johannesburg, Johannesburg, South Africa, from October 2016 to February 2018. Since March 2018, he has been with the Department of Energy Technology, Aalborg University, Esberg, Denmark, as the faculty member. He has authored 250 plus scientific papers.

Dr. Padmanaban has received the Best Paper cum Most Excellence Research Paper Award of IET-SEISCON'13, IET-CEAT'16, and five Best Paper Awards from ETAEERE'16 sponsored Lecture note in Electrical Engineering, Springer book series. He serves as an Editor/Associate Editor/Editorial Board in many refereed journal, in particular the IEEE TRANSACTION ON POWER ELECTRONICS, the IEEE SYSTEMS JOURNAL, Subject Editor of the *IET Renewable Power Generation*, the *IET Power Electronics*, the *IET Generation, Transmission and Distribution*, and the IEEE ACCESS. He was an involved member on invitation with various capacities in the committee for more than 4500 plus various international conferences including the IEEE and IET.

Pandav Kiran Maroti (S'16) received the Bachelor's degree in electronics and telecommunication from Dr. Babasaheb Ambedkar Marathwada University, Aurangabad, India, in 2011, and the Master's of Technology degree in power electronics and drives with distinction from the Vellore Institute of Technology, Vellore, India, in 2014. His Ph.D. theses focused in the field of power electronics and was successfully submitted with the University of Johannesburg, South Africa in April 2018.

He was working as an Assistant Professor with the Marathwada Institute of Technology during 2014–2016. He is currently Associated with the Department of Electrical and Electronics Engineering, Marathwada Institute of Technology, Aurangabad, India. He has published scientific papers in the field of power electronics (multilevel dc–dc and dc–ac converter, multiphase open winding inverter).

Dr. Maroti is an editorial and reviewer member of various international journal and conferences.

Amarjeet Kumar Sharma received the B.E. degree in electrical engineering from the Muzaffarpur Institute of Technology, Muzaffarpur, India, in 2010, and the M.Tech. degree in electrical engineering (power system) from the Maulana Abul Kalam Azad University of Technology, Bidhan Nagar, West Bengal, in 2016.

He has published various papers in international journal and attended workshop/conferences on renewable energy and modern trends in electrical power system. He is currently an Assistant Professor with the Department of Electrical Engineering, Millia Institute of Technology, Purnea, India. His research areas include renewable energy and electrical machine.